Coincidence method for measuring the mass of neutral fragments emitted in a delayed fragmentation process from a singly charged molecule: Fragmentation pathway of adenine

S. Martin, R. Brédy, A. R. Allouche, J. Bernard, A. Salmoun, B. Li, and L. Chen
Université Lyon 1, CNRS, LASIM UMR 5579, 43 Boulevard du 11 Novembre 1918, F-69622 Villeurbanne, France
(Received 11 December 2007; published 23 June 2008)

We have studied by mass spectrometry the fragmentation pathways of a molecule of biological interest: adenine $H_5C_5N_5$ (Ad). The adenine molecules are ionized and excited in a single collision event mode with slow highly charged Ar^{8+} ions. A method based on the detection in coincidence of neutral and charged fragments has been developed for studying delayed fragmentation channels. The measured spectra show that the well-stated process, i.e., the successive emission of HCN fragments, is not the only fragmentation pathway. Although in the first fragmentation step the dominant channel is the emission of a neutral HCN^0 (88%), in the second fragmentation step the branching ratios for the delayed emission of an HCN^0 and an H_2CNCN^0 from the intermediate parent ion $H_4C_4N_4^+$ [$(Ad\text{-}HCN)^+$] are surprisingly similar, 54% and 46%, respectively. As a consequence, the role of these two latter channels in the reversal process, i.e., the formation of adenine in gas phase, should be considered. *Ab initio* calculations of molecular energies show that the energy levels of these two fragmentation channels are very close. This is in qualitative agreement with the measured comparable branching ratios.

DOI: 10.1103/PhysRevA.77.062513 PACS number(s): 33.15.Ta, 34.70.+e, 95.30.Ft

I. INTRODUCTION

Formation and fragmentation of nucleic acid bases have drawn attention from broad scientific communities such as chemistry, physics, astrobiology, and biology [1–3]. Productions of amino acids or complex oligomers have been investigated in laboratory experiments as well as in theoretical simulations [4,5]. Gas phase studies are of significance for understanding and determining properties of these nucleic acid bases. Fragmentation studies of labeled adenine or protonated adenine have received constant attention using a large panel of mass spectrometry (MS) techniques and various ionization and excitation methods. In the first mass spectra of fragmented adenine [6,7], the sequential loss of HCN molecules has been well identified. In the more recent mass spectra of labeled adenine using ^{15}N, ^{13}C, and D, the location of the emitted HCN fragment has been studied [8,9], showing that the loss of the first HCN involves principally N-1 and C-2. Figure 1 shows the structure and labeling of the constituents of adenine. Other fragmentation channels such as the emission of NH_3 and NH_2CN neutral fragments and of NH_4^+ charged fragment have also been observed recently in collision-induced dissociation (CID) of protonated adenine with Tandem mass spectroscopy [3].

The formation and the existence of nucleobases or amino acids in an interstellar medium have been discussed in recent papers [5,10]. To investigate under laboratory conditions the possible existence of such molecules in an astrophysical context, photoionization mass spectroscopy has been investigated in synchrotron radiation experiments [11]. In the 6–22 eV photon energy region, the appearance energies (AE) of photoions from adenine have been measured and used to explain the fragmentation patterns. The AE of $C_nH_nN_n^+$ ($n=5,4,3,2$) ions were found to be 8.2, 11.56, 12.8, and 13.7 eV, respectively. The steady increase of these AE is consistent with a successive emission model, i.e., the loss of an extra HCN neutral fragment requires an excess energy of 3.4, 4.5, and 5.4 eV from the respective parent ions. These results suggest that the nucleobases can be easily photodissociated in environments where the uv radiation is intense and their existence in the interstellar medium is possible only in regions where radiation protection is effective. The formation mechanisms of the nucleobases in protected regions are also a matter of controversy [4,12]. In particular, the formation of adenine in four successive steps by assembling only the HCN molecules seems to be theoretically improbable under typical protected interstellar conditions at low temperature (10–100 K). Indeed, to get more insight into the formation mechanism of a molecule, it is relevant to investigate all possible channels of the reverse process, i.e., fragmentation, especially for channels with low dissociation energy. These low-energy-cost channels could more likely be activated in a cold environment, namely in interstellar molecular clouds.

In a recent paper, Alvarado *et al.* [13] studied the decay of gas phase singly charged adenine excited by the impact of slow neutral projectile He^0 (keV energies). In collisions using slow highly charged projectiles, for example Ar^{8+}, charged adenine molecules have also been measured [14]. In such interactions, the ionization of the molecule is based on resonant electron transfer from the adenine molecule to the projectile ion. At large impact distance, the excitation of the molecule is due to the heating of the electron cloud via electronic interaction between the projectile and the target. Sin-

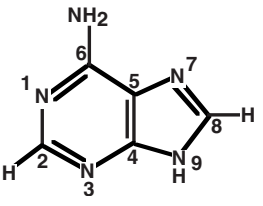

FIG. 1. Structure of the adenine molecule and labeling of its constituents.

gly and doubly charged adenine with low internal excitation energy can be produced via the capture of one or two electrons. From correlation spectra between charged fragments, detailed fragmentation schemes of doubly charged Ad^{2+} parent ions have already been measured [14].

In this paper, we report on the fragmentation pattern of singly charged adenine formed in collisions between Ar^{8+} and adenine. Delayed fragmentation channels corresponding to the ejection of a neutral fragment have been observed in time-of-flight (TOF) correlation spectra using a single TOF tube. TOF correlations between the charged and neutral fragments have been simulated with the SIMION software [15]. The TOF analysis of the neutral fragment has been possible owing to a special electric field design with multiple sections between the acceleration region of the recoil ions and the TOF tube. The branching ratios for the emission of neutral fragments from $C_5H_5N_5^+$ and $C_4H_4N_4^+$ parent ions have been measured. In addition to the well-known successive emission of HCN fragments, direct emission of other neutral fragments has been observed. To explain tentatively the experimental results, density-functional theory (DFT) calculations have been performed using the GAUSSIAN 98 package [16] for adenine and the main fragment molecules in various transition states, like 1,3,5 triazine ($C_3H_3N_3$), HCN^0 and the dimer of HCN.

II. EXPERIMENT

The experimental setup used in this work has been described in detail elsewhere [17,18]. In short, Ar^{8+} ions are produced in a NanoGan 3 electron cyclotron resonance (ECR) ion source and extracted at 56 keV. The size of the incoming Ar^{8+} beam is reduced using a small aperture (diameter 300 μm) placed just before the interaction region. The target is an effusive jet of adenine prepared by evaporating an adenine powder (Sigma Aldrich, purity 99%) in an oven at 130 °C. The spectroscopy studies of several tautomeric forms of adenine showed that at this temperature, only one tautomer is present at more than 99% [19]. The adenine jet is set perpendicularly to the ion beam and collimated by an aperture of 1 mm in diameter. The background gas pressure in the collision chamber was maintained below 2×10^{-9} mbar during the experiment.

Electrons and recoil ions including stable singly and doubly charged adenine and ionized fragments are extracted by a transverse electric field of 500 V/cm applied between two extraction plates separated by 8 mm and set to +800 and +400 V, respectively. Mapping of equipotential lines for the extraction, acceleration, focusing, and steering regions and for the free flight region on the TOF tube is shown in Fig. 2. Except for the extraction plates, all electrodes have cylindrical symmetry. After the extraction field, the ions are accelerated over 7 mm until the cone-shaped electrode, which is biased to −2000 V. The TOF tube of length 837 mm is set to the same potential, −2000 V. Between the cone and the TOF tube, the einzel lens and the steerers are used to focus and to steer the recoil ions in order to improve the collection efficiency through the TOF tube. The einzel lens is composed of three ring electrodes; the first and the third ones are biased to

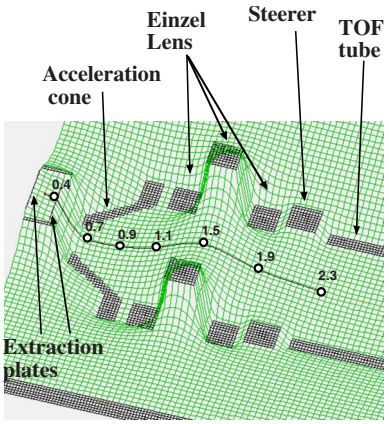

FIG. 2. (Color online) Mapping of the equipotential lines for the extraction, acceleration, and focalization electric fields. The bold curve represents the field line along the trajectory of the ion. The number beside each circle denotes the time in μs when an Ad^+ ion passes through different regions. 0–0.4 μs: extraction field; 0.4–0.7 μs: acceleration field; 0.7–0.9 μs: cone; 1.1–1.9 μs: lens; 1.9–2.3 μs: steerers. The region between the lens and the steerers is a special region with small potential gradient and where the potential value is close to that applied on the TOF tube.

−2000 V, the central one to +1710 V. The steerers are set to −1420 V. A special region of low potential gradient from the central electrode of the einzel lens to the entrance of the TOF tube presents a particular interest for studying delayed emission of neutral fragments. Due to the low potential gradient just before the TOF tube, the velocity of fragments including neutrals produced in this weak electric field is only slightly different from that of the parent ions. Delayed fragmentation processes in this region can then be assigned by the correlation of the modified TOF of the fragments. At the end of the TOF tube, a position-sensitive detector composed of two multichannel plates and a multianode are used to detect the recoil ions and fragments. To increase the detection efficiency, the ions are post-accelerated with a voltage of 3.4 keV toward the detector. Electrons ejected during the collision are extracted, accelerated, and detected by a passivated implanted planar silicon (PIPS) detector (not shown in Fig. 2). After the interaction, the final charge of the scattered projectile is analyzed by a cylindrical analyzer (also not shown in Fig. 2). In the present experiment, Ar^{7+} outgoing projectiles are selected. Coincidence measurements between Ar^{7+}, the recoil adenine ions, and the ejected electrons are performed in an event-by-event mode. The initial charge state r of the parent adenine ion is determined unambiguously for each fragmentation event with $r=1+n$, n standing for the total number of transferred and ejected electrons.

III. EXPERIMENTAL RESULTS AND DISCUSSION

Events corresponding to the relaxation of monocharged adenine Ad^+ parent ions are selected with the criterion such that $n=0$, i.e., no electron is detected. The contribution to the raw spectrum from Ad^{2+} parent ions characterized by the ejection of one electron $n=1$ was possible due to the limited electron detection efficiency. It was corrected following the

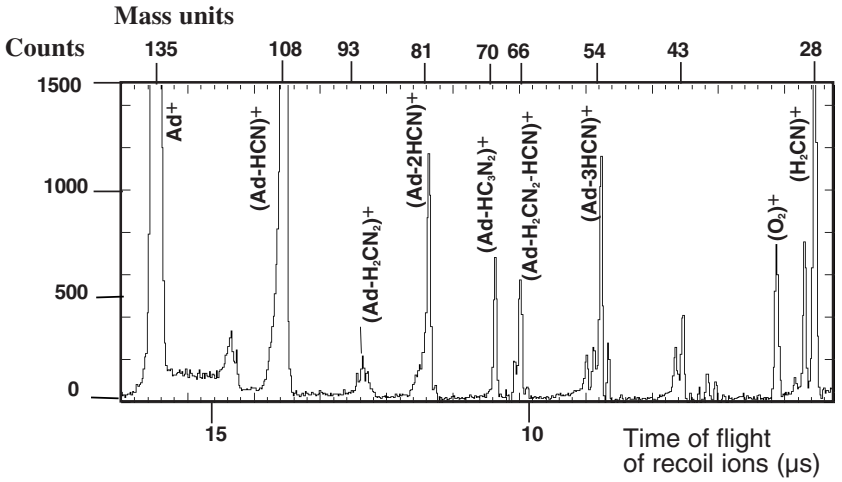

FIG. 3. One-dimensional TOF fragmentation spectrum of singly charged adenine parent ions due to the impact of Ar^{8+}. The events are selected by the detection of a scattered Ar^{7+} with the electron number criterion, $n=0$. The spectrum is calibrated in mass as shown in the upper scale.

standard procedure given in Ref. [17]. The measured recoil ion TOF spectrum related exclusively to the $Ar^{8+}+Ad \rightarrow Ar^{7+}+Ad^{+*}$ primary reaction is shown in Fig. 3. All the peaks in this spectrum result from the decay of singly charged parent ions Ad^+. The high abundance of the intact Ad^+ ($m=135$) and $(Ad\text{-}HCN)^+$ ($m=108$) peaks shows that these charged molecules are preferentially produced with high stability in the one-electron capture process. The single-capture cross section has been estimated to about 2.2×10^{-14} cm^2 [14] corresponding to an impact parameter of about 15 Å, much larger than the radius of the molecule of about 5 Å. In such long-range collisions, the molecules are prepared in low excitation energy states [14]. Other peaks of the spectrum are mainly products of the emission of neutral fragments, as will be discussed below.

Table I presents the measured branching ratios of the main decay channels from Ad^+ by the ejection of one neutral fragment. The major channel (mass 108) is attributed to the emission of a HCN^0 as observed in many experiments [6–9]. Minor channels (mass 93 and 70) are attributed to the emission of $H_2CN_2^0$ or $HC_3N_2^0$ fragments, respectively. Details about these channels can be found in Ref. [11].

In Fig. 3, The peak H_2NC^+ is explained by the emission of C-6 NH_2, where the charge is carried out by the small fragment. Other peaks ($m=81,66,54,\ldots$) are mainly due to the ejection of two or three neutral fragments in a multistep process. Although the identification of peaks of the final charged fragments like $(Ad\text{-}2HCN)^+$ or $(Ad\text{-}3HCN)^+$ is unambiguous, little experimental evidence can be extracted from this one-dimensional TOF spectrum concerning the dynamical information of the fragmentation process. For example, from this spectrum, it is not possible to tell if the peak $m=81$ is due to the successive loss of 2 HCN fragments or due to the direct emission of one fragment $H_2C_2N_2$. An intriguing part of this spectrum is that between Ad^+ and $(Ad\text{-}HCN)^+$ peaks. A plateau much higher than the background noises extends from the Ad^+ peak to a TOF of about 16 μs. A similar plateau slightly higher than the mean background noise is also notable between the $(Ad\text{-}HCN)^+$ and $(Ad\text{-}H_2CN_2)^+$ peaks. These two plateaus are discussed in more detail below.

TABLE I. Branching ratios for the emission of a neutral fragment from the singly charged adenine for the first step of the dissociation scheme.

First step	HCN	H_2CN_2	HC_3N_2
Counts	23376	1380	1872
Branching ratios	0.88	0.05	0.07

Figure 4 shows a correlation spectrum for events where two or more fragments are detected in a single collision. The TOF of the last detected fragment is plotted along the horizontal axis and the TOF of the other fragments along the vertical axis. This spectrum was recorded without any electron number selection criterion, in other words, without selection of the parent ion charge state. Attribution of the main spots was presented in Ref. [14]. For instance, the spots characterized by two fragments of mass (107-28) and (92-43) are due to the fission of doubly charged parent adenine ions that have lost a small charged fragment, H_2CN^+ and $H_3CN_2^+$, respectively. Other spots like (80-28) and (65-43) are mainly due to the emission of additional HCN^0 fragments. Several spots in this spectrum present a long tail leaned to the right-hand side with a shorter TOF for the heavy fragment and a longer TOF for the light one comparing, respectively, to their nominal TOF. This feature is a typical signature of the delayed fission process of Ad^{2+} that occurs mainly in the extraction region in a time range shorter than 0.4 μs from the collision time. In fact, in a delayed fission process, the singly charged heavy fragment arriving at the entrance of the TOF tube is slightly faster than those produced in a prompt dissociation process. It has been accelerated during a short time before the fragmentation as a part of the doubly charged parent ion that has a larger charge to mass ratio than the fragment. Conversely, due to its larger charge over mass ratio than the parent ion, the singly charged light fragment resulting from a delayed dissociation in the extraction field is slightly slower at the entrance of the TOF tube than those produced in a prompt dissociation process. It is notable that the tail of the spot (107-28) could be extended following a continuous curved line to join a short tail from another spot close to the diagonal of the spectrum at the TOF of Ad^{2+}. This curved line corresponds to the delayed fragmentation all along the trajectory of the molecular ions from $t=0$ in the

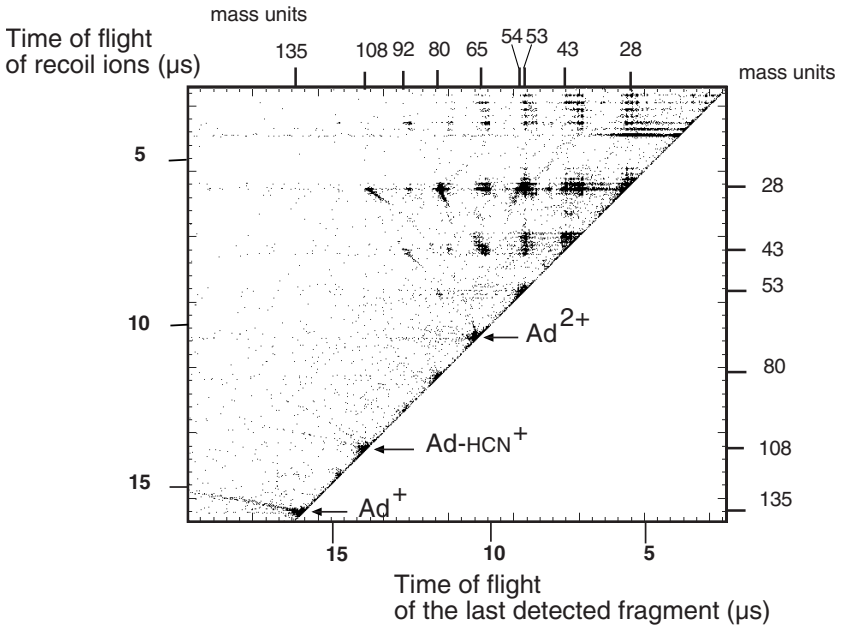

FIG. 4. Correlation spectrum between fragments resulting from the dissociation of a singly or doubly charged adenine parent ion. This spectrum was recorded without the electron number selection condition.

collision region to the time when the parent molecule arrives at the entrance of the TOF tube.

The spot labeled Ad^{2+} in Fig. 4 results mainly from delayed fission processes occurring on a larger time scale that allows the parent ions to arrive inside the TOF tube before fragmenting. The two fragments are therefore detected with the same TOF and can be discriminated only by their positions on the detector. Using a multipixel detector with high multihit capability, these events are well detected and recorded. The part of the tail attached to the Ad^{2+} spot is attributed to the delayed fission during the passage through the special region with low potential gradient between the central lens and the entrance of the TOF tube (1.6–1.8 μs). In such cases, the TOF for the light and heavy singly charged fragments are slightly modified comparing to the TOF of Ad^{2+}.

In an analogous way, the intense spots of Ad^+ and $(Ad\text{-}HCN)^+$ with mass 135 and 108 (Fig. 4) are explained, respectively, by delayed fragmentation inside the TOF tube of the initial parent ions Ad^+ and that of the intermediate parent ions $(Ad\text{-}HCN)^+$. However, in the present cases one of the fragments is neutral. Due to the acceleration field, the kinetic energy of the singly charged parent is 2.6 keV. After the dissociation, the neutral carries a part of the energy that is enough to produce electrons on the surface of the multichannel plate (MCP) detector placed at the end of TOF tube and therefore to lead to a sufficient detection efficiency. These two spots present also long tails. As in the case of the Ad^{2+} spot, they are attributed to delayed fragmentation in the low potential gradient region before the entrance of the TOF tube. In this region, the electric potential decreases along the ion trajectory (Fig. 2) and the ions are accelerated. At any position on this potential slope, if a neutral fragment is lost, it is no longer accelerated and starts to drift with a constant velocity. Its total TOF, therefore, should be slightly longer than the TOF of the parent ion that is continuously accelerated along the slope until the entrance of the TOF tube. On the other hand, the residual charged fragment goes down the potential slope with a smaller mass than the parent ion. So, its TOF should be shorter than that of the parent ion. The shape of the tails in Fig. 4 corresponds qualitatively well to the differentiated TOF of the two dissociation partners. The delayed dissociation along the potential slope allows us to interpret also the plateau observed beside the Ad^+ peak on the one-dimensional TOF spectrum (Fig. 3). This plateau corresponds to the TOF of the residual charged fragment in

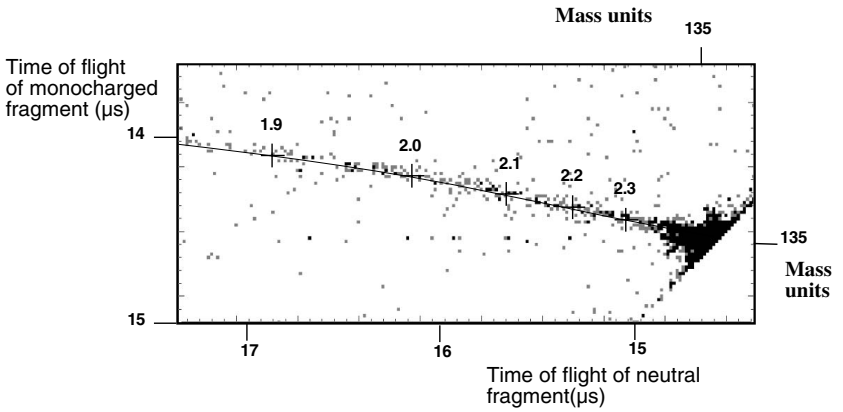

FIG. 5. Expanded region of correlation spectrum around the spot Ad^+ (m=135). Crosses: correlated TOF of neutral and charged fragments simulated with the SIMION code for the delayed fragmentation channel $Ad^+ \rightarrow (Ad\text{-}HCN)^+ + HCN$ in a time range 1.9–2.3 μs.

TABLE II. Branching ratios for the emission of a neutral fragment from the intermediate parent ion $(Ad\text{-}HCN)^+$.

Second step	HCN	H_2NCCN
Counts	64	56
Branching ratios	0.54	0.46

the delayed dissociation processes. By comparison, in the same TOF window, of the event counts of this plateau (Fig. 3) and of the tail attached to the spot Ad^+ in Fig. 4, we have estimated the detection efficiency of the neutral fragment to be about 15%.

The parts of the spectrum around the spots Ad^+ and $(Ad\text{-}HCN)^+$ of Fig. 4 are presented in Figs. 4 and 5, respectively. To assign the delayed dissociation channels without ambiguity, ion trajectory simulations have been performed with the SIMION software [15] for delayed fragmentation that occurs from 100 ns to 2.3 μs after the collision.

In the case of Ad^+ parent ions, the tail of the spot Ad^+ is well reproduced by the delayed dissociation channel $Ad^+ \rightarrow (Ad\text{-}HCN)^+ + HCN^0$. The calculated TOF of the two fragments are plotted in Fig. 4 for the delayed fragmentation time from 1.9 to 2.3 μs. The good agreement between the simulation and the experimental observation confirms that the dominant delayed fragmentation channel of Ad^+ is the ejection of a HCN^0. Along the trajectory of ions from the extraction field to the TOF tube, several acceleration and deceleration regions can be distinguished (Fig. 1). Starting by a smooth acceleration due to the low extraction field strength, the ions are strongly accelerated to the bottom of the potential curve inside the conic electrode. Due to the potential saddle established with the high positive potential of the central lens electrode, the ions are decelerated and then accelerated through a low potential gradient region before entering in the field-free region of the TOF tube. The simulation shows that the position of the fragmentation along the trajectory is crucial for the observation of the tail in the correlation spectrum. Only fragmentations that occur just before the TOF tube in the time region 1.9–2.3 μs can contribute to its formation. This region is characterized first by a potential close to that of the tube (−2000 V) so that the neutral has sufficient kinetic energy to be detected and the TOF of the two fragments do not differ too much from that of the parent ion. Second, due to the low potential gradient, the delayed fragmentation could be observed over a relatively long time window, namely 0.4 μs (=2.3–1.9 μs).

In Fig. 5, close to the spot $(Ad\text{-}HCN)^+$ and in spite of poor statistics, two tails are observed. Simulations have been performed to reproduce these two tails for delayed fragmentation from 1.7 to 2 μs. One tail, denoted *A*, is attributed to the emission of HCN^0. This channel is consistent with the well-established knowledge on the successive emission of HCN units. The other one, denoted *B*, reveals an unexpected channel attributed unambiguously to the fragmentation of intermediate parent ions $(Ad\text{-}HCN)^+$ ($H_4N_4C_4^+$, $m=108$) into two fragments of the same mass $H_2N_2C_2 + H_2N_2C_2^+$ ($m=54$). The number of counts in each tail is proportional to the decay rate from the same parent state $H_4N_4C_4^+$ to the corresponding fragmentation channel and to the population difference of the parent ions in the time window of the measurement (from 1.7 to 2 μs). From the ratio of the two measured count numbers, we obtained the ratio between the decay rates, and therefore the relative branching ratios of the two delayed dissociation channels (Table II). Nearly equal probabilities have been found for the emission of HCN^0 and $H_2N_2C_2^0$ fragments from $(Ad\text{-}HCN)^+$. This result means that in the one-dimensional TOF spectrum (Fig. 2), the peak assigned to $(Ad\text{-}3HCN)^+$ ($m=54$) results from two decay channels. The first one is a three-step process including the successive emission of three HCN^0 via the intermediate molecules, $(Ad\text{-}HCN)^+$ and $(Ad\text{-}2HCN)^+$. The second one is a two-step process including a prompt emission of HCN and

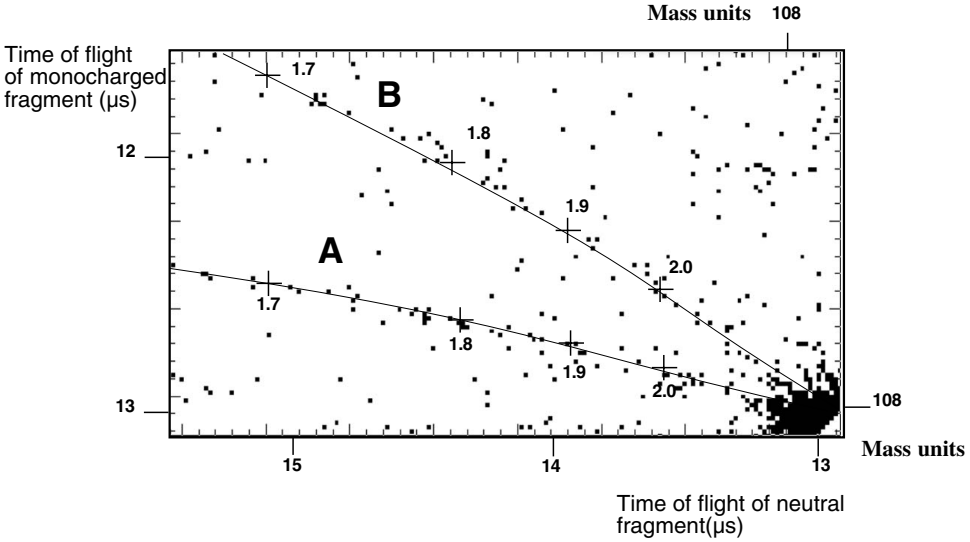

FIG. 6. Expanded region around the spot $(Ad\text{-}HCN)^+$ ($m=108$). Two tails are observed. Crosses: simulation of the correlated TOF of the neutral and charged fragments for two delayed decay channels from the intermediate $(Ad\text{-}HCN)^+$ parent ions. Tail A: reaction $(Ad\text{-}HCN)^+ \rightarrow (Ad\text{-}2HCN)^+ + HCN^0$, $108 \rightarrow 81+27$. Tail B: reaction $(Ad\text{-}HCN)^+ \rightarrow (Ad\text{-}3HCN)^+ + H_2C_2N_2^0$, $108 \rightarrow 54+54$. Simulations have been performed for delay times, 1.7–2.0 μs from the collision time.

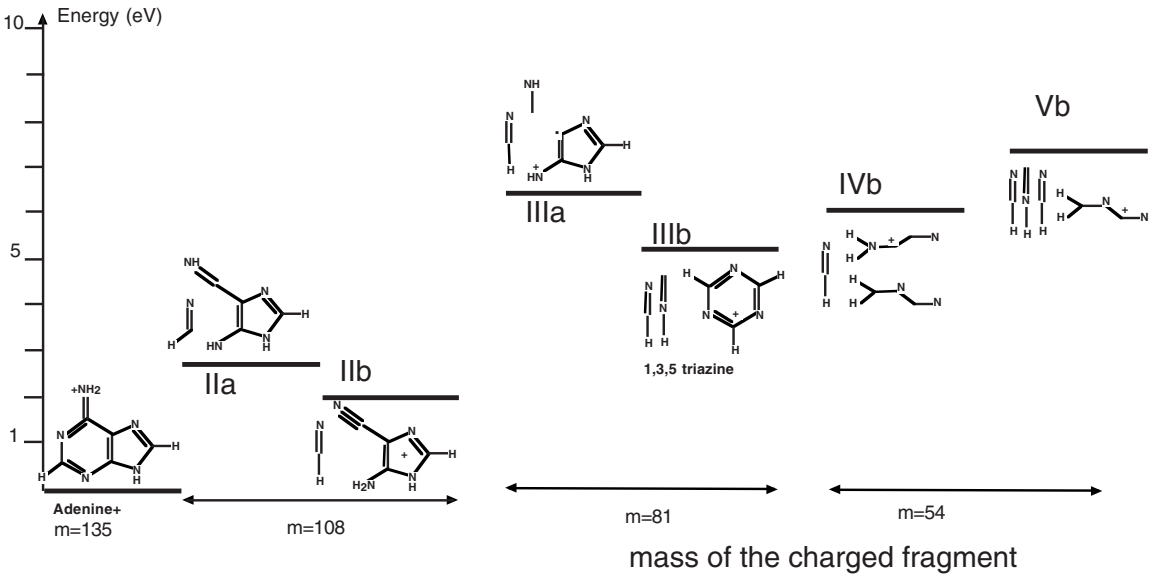

FIG. 7. Energy levels or fragmentation decay routes for Ad^+.

a delayed emission of $H_2C_2N_2$ from $(Ad\text{-}HCN)^+$.

In order to explain tentatively the measured decay branching ratios of the intermediate parent ions $(Ad\text{-}HCN)^+$, DFT calculations using a Becke three-parameter Lee-Yang-Parr hybrid functional with 6-31G basis set [16] have been performed to estimate the energy levels of several decay channels. Following the notation of Fig. 5 in [11], the calculated energy level of Ad^+, the intermediate energy level of $(Ad\text{-}HCN)^+ + HCN^0$ denoted IIa, the intermediate energy level of $(Ad\text{-}2HCN)^+ + 2HCN^0$ denoted IIIa, the energy level of $(Ad\text{-}3HCN)^+ + H_2CNCN^0 + HCN^0$ denoted here IVb, and the energy level of $(Ad\text{-}3HCN)^+ + 3HCN^0$ denoted here Vb are all presented Fig. 6. The energy levels of IIIa and IVb are very close with a little difference of about 0.4 eV. This is inconsistent with the measured comparable branching ratios (Table II) for these two decay channels from the intermediate parent ions $(Ad\text{-}HCN)^+$. The energy level of the channel with the same final charged products $(Ad\text{-}3HCN)^+$ from the emission of three HCN fragments is more than 1 eV higher than the channel IVb (see Fig. 7). Therefore, it can be opened at higher internal excitation energy only.

IV. CONCLUSIONS

In conclusion, a method for studying the fragmentation pathways of singly charged adenine has been developed. Due to the special electric-field structure upstream of the TOF tube, neutral fragments emitted about 2 μs after the collision from the initial parents Ad^+ or from the intermediate parents $(Ad\text{-}HCN)^+$ have been measured in coincidence with the residual singly charged fragment. Using this method, we have provided experimental evidence for a delayed fragmentation channel in the decay chain of the adenine, i.e., the emission of a H_2CNCN^0 fragment from the intermediate parents $(Ad\text{-}HCN)^+$. The absence of this channel in the current knowledge on the decay of adenine is not surprising: with the generally used one-dimensional TOF analysis method, this channel overlaps with that of the successive emission of three HCN^0 fragments. The coincidence detection of both the charged and neutral fragments is essential in the identification of such a decay channel. This channel has been found with a comparable branching ratio to that of the HCN emission channel. The competition between these two channels has been interpreted tentatively by the very similar dissociation energies given by *ab initio* calculations. This low-energy-delayed fragmentation channel suggests a possible scheme in the reverse process, the formation of *adenine*, especially the formation of *adenine* in the interstellar medium. Processes involving not only an oligomerization of the HCN molecule but also other more complex mechanism such as the bond of two $H_2C_2N_2$ molecules should be considered.

[1] A. Brack, Chem. Biodivers. **4**, 665 (2007).
[2] Z. Peeters, O. Botta, S. B. Charnley, R. Ruiterkamp, and P. Ehrenfreund, Astrophys. J. Lett. **593**, L129 (2003).
[3] C. C. Nelson and J. A. McCloskey, J. Am. Chem. Soc. **114**, 3661 (1992).
[4] I. W. M. Smith, D. Talbi, and E. Herbst, Astron. Astrophys. **369**, 611 (2001).
[5] R. Glaser, B. Hodgen, D. Farrelly, and E. McKee, Astrobiology **7**, 455 (2007).
[6] J. S. Shannon and D. S. Letham, NZJ. Sci. **9**, 833 (1966).
[7] J. M. Rice and G. O. Dudek, J. Am. Chem. Soc. **89**, 2719 (1967).
[8] M. D. Carmen, G. Barrio, J. C. D. Scopes, J. B. Holtwick, and N. J. Leonard, Proc. Natl. Acad. Sci. U.S.A. **78**, 7, 3986

(1981).
[9] S. K. Sethi, S. P. Gupta, E. E. Jenkins, C. W. Whitehead, L. B. Townsend, and J. A. McCloskey, J. Am. Chem. Soc. **104**, 3350 (1982).
[10] Y. J. Kuan, S. B. Charnley, H. C. Huang, W. L. Tseng, and Z. Kisiel, Astrophys. J. **593**, 848 (2003).
[11] H. P. Jochims, M. Schwell, H. Baumgärtel, and S. Leach, Chem. Phys. **314**, 263 (2005).
[12] S. Chakrabarti and S. K. Chakrabarti, Astron. Astrophys. **354**, L6 (2000).
[13] F. Alvarado, S. Bari, R. Hoekstra, and T. Schlatölter, J. Chem. Phys. **127**, 034301 (2007).
[14] J. Bernard, R. Brédy, L. Chen, S. Martin, and B. Wei, Nucl. Instrum. Methods Phys. Res. B **245**, 103 (2006).
[15] SIMION 7, Ion Source Software.
[16] M. J. Frisch, G. W. Trucks, H. B. Schlegel, G. E. Scuseria, M. A. Robb, J. R. Cheeseman, V. G. Zakrzewski, J. A. Montgomery Jr., R. E. Stratmann, J. C. Burant, S. Dapprich, J. M. Millam, A. D. Daniels, K. N. Kudin, M. C. Strain, O. Farkas, J. Tomasi, V. Barone, M. Cossi, R. Cammi, B. Mennucci, C. Pomelli, C. Adamo, S. Clifford, J. Ochterski, G. A. Petersson, P. Y. Ayala, Q. Cui, K. Morokuma, D. K. Malick, A. D. Rabuck, K. Raghavachari, J. B. Foresman, J. Cioslowski, J. V. Ortiz, A. G. Baboul, B. B. Stefanov, G. Liu, A. Liashenko, P. Piskorz, I. Komaromi, R. Gomperts, R. L. Martin, D. J. Fox, T. Keith, M. A. Al-Laham, C. Y. Peng, A. Nanayakkara, C. Gonzalez, M. Challacombe, P. M. W. Gill, B. Johnson, W. Chen, M. W. Wong, J. L. Andres, C. Gonzalez, M. Head-Gordon, E. S. Replogle, and J. A. Pople, *Gaussian 1998* (Gaussian inc., Pittsburgh, 1998).
[17] S. Martin, L. Chen, R. Brédy, J. Bernard, M. C. Buchet-Poulizac, A. Allouche, and J. Désesquelles, Phys. Rev. A **66**, 063201 (2002).
[18] L. Chen, B. Wei, J. Bernard, R. Brédy, and S. Martin, Phys. Rev. A **71**, 043201 (2005).
[19] P. Colarusso, K. Zhang, B. Guo, and P. F. Bernath, Chem. Phys. Lett. **269**, 39 (1997).